Limited Precision of Lumbar Spine Dual-Photon Absorptiometry by Variations in the Soft-Tissue Background

Roelf Valkema, Luis F. Verheij, Jacobus A.K. Blokland, Aeilko H. Zwinderman, Olav L.M. Bijvoet, Socrates E. Papapoulos, and Ernest K.J. Pauwels

Department of Diagnostic Radiology, Division of Nuclear Medicine, Department of Endocrinology, Clinical Investigation Unit, and Department of Medical Statistics, University Hospital, Leiden, The Netherlands

The estimation error due to variations in soft-tissue baseline in lumbar bone mineral content (BMC) measured by dual-photon absorptiometry (DPA) was calculated with a new method of automatic baseline subtraction. In water phantom measurements, the s.d. of the soft-tissue (ST) baseline matched closely (r = 0.98) to the random error, calculated using 44 keV and 100 keV count rates and the directly determined baseline variations. In 21 volunteers and in 70 patients with osteoporosis, the ST variations were larger than the expected random error, revealing a source of error related to the inhomogeneity of soft tissue. The estimation error in BMC caused by ST variations was 0.7% in healthy subjects (mean BMC 40.5 gHA) and 1.5% in patients (mean BMC = 26.4 gHA). These results indicate that ST-related errors are an important limit to the precision of lumbar DPA measurements.

J Nucl Med 1990; 31:1774–1781

Osteoporosis is a major health problem with various treatments and preventive regimens currently under intensive investigation (*1*). For the assessment of the efficacy of these interventions, the fracture incidence and the changes in bone mass must be longitudinally evaluated. Changes in bone mass induced either by natural bone loss or by therapeutic interventions are relatively small (*2*) and measurements of high reproducibility are essential (*3,4*). Dual-photon absorptiometry (DPA) measurements of the lumbar spine bone mineral content (BMC) or bone mineral density (BMD) are widely used, but the reproducibility of this technique does not allow the assessment of timed changes in the individual patient reliably. Various sources of error affecting the reproducibility of DPA have been investigated previously, related to the equipment used or to the patient (*5–10*).

A number of studies mention inhomogeneity of soft tissue (ST) as a source of accuracy error (*11–15*). The extent, however, to which this may affect the reproducibility of DPA measurements is not known. The only study in which the reproducibility error due to inhomogeneity of soft tissue was investigated was performed by Krølner, who proposed a fat inhomogeneity index based on subjective reading of the individual scan profiles by the operator (*13*).

In the present study, we have used an automatic and objective method to quantify the effect of the variations in ST attenuation on the reproducibility of DPA measurements of the lumbar spine in normal subjects and in patients with osteoporosis.

PATIENTS AND METHODS

Dual-Photon Absorptiometry: Data Acquisition

Dual-photon absorptiometry was performed with a Novo BMC-LAB22a (Novo Diagnostic Systems, Bagsvaerd, Denmark) densitometer, using acquisition software version 1 with a Hewlett Packard (Corvallis, OR) HP-85 microcomputer. The scanning speed is 0.4 cm/sec, the scan interval is 0.4 cm, and the sampling interval is 1 sec, resulting in image pixels of 0.4 cm by 0.4 cm. The software with this bone densitometer uses a rearranged formula to calculate BMC (*12,16*). In this method, I^0_{44} and I^0_{100}, equivalents of the unattenuated photon beams of 44 keV and 100 keV, are the detected intensities of the beam in both channels with attenuation by ST only, measured at a point next to the spine. The general equation for calculation of bone mineral mass can be written as follows:

$$M_{Bone}(x,y) = \frac{\ln(I^0_{44}/I_{44}) - RST \times \ln(I^0_{100}/I_{100})}{\mu_{Bone:44} - RST \times \mu_{Bone:100}}, \quad (1)$$

where M_{Bone} (x,y) is the bone density (g/cm^2) at a point corresponding to pixel with location (x,y) in the BMC image and I_{100} and I_{44} are the measured photon intensities for that point. RST equals $\mu_{ST:44}/\mu_{ST:100}$, which denotes the ratio of attenuation of the two photon energies in ST, while $\mu_{Bone:44}$, $\mu_{ST:44}$, $\mu_{Bone:100}$ and $\mu_{ST:100}$ are the mass attenuation coefficients for bone mineral and ST at the low and high energies, respec-

Received Nov. 18, 1989; revision accepted Apr. 13, 1990.

For reprints contact: R. Valkema, MD, Division of Nuclear Medicine, Building 1, C4-Q, University Hospital, PO Box 9600, 2300 RC Leiden, The Netherlands.

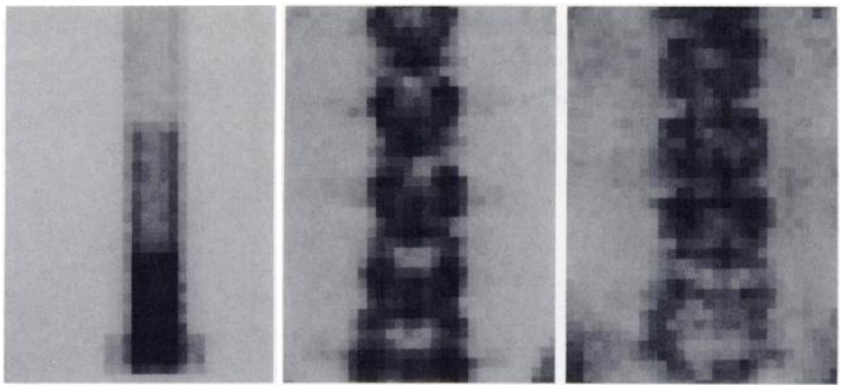

FIGURE 1
Display of DPA scans of an aluminium phantom immersed in 16 cm water (left), the lumbar spine of a healthy subject (middle), and the lumbar spine of a patient with osteoporosis (right). Note the homogeneous appearance of the water background in the phantom study, in contrast to the more variable soft tissue background in the healthy subject and the patient.

tively. The value of RST is fixed at 1.41 in the program of the densitometer (*12*). Rearranging the above formula gives:

$$M_{Bone}(x,y) = \frac{C_2}{C_1} \times \{1.41 \times \ln(I_{100}) - \ln(I_{44})\}$$

$$- \frac{C_2}{C_1} \times \{1.41 \times \ln(I^0_{100}) - \ln(I^0_{44})\}, \quad (2)$$

where the constant C_1 is the denominator of Equation 1 and a constant C_2 acts as a scaling factor to yield pixel values between 1 and 255, which are convenient for storage as byte mode data and for display on a monitor. The constant C_2 also includes a correction for the size of the pixels (0.16 cm^2). The acquisition data thus represent BMC for each pixel, after a preliminary subtraction of the soft-tissue component. These scaled pixel values (U) have the dimension grams of hydroxyapatite (gHA).

Calculation Methods

The acquisition data were transported to a general purpose nuclear medicine computer system (Medical Data Systems A^2, Ann Arbor, MI) for further evaluation. The data were displayed as a density image on the screen of a grey scale monitor (Fig. 1).

The calculation program used in the present study performs essentially the same calculations as the original program, but differs from the original in two respects. First, the region of interest (ROI) is a rectangle of variable size placed by the operator on the complete image instead of setting the delimiters in each scan line separately (*17*). The rectangular ROI includes the vertebral bodies L2 through L4 (Fig. 2). Second, our program allows automatic calculation of the final ST baseline subtraction. This automated calculation procedure is aimed at the selection of those paravertebral baseline values that are representative for the ST inside the ROI and exclusion of the extreme high and extreme low values. Parts of the background containing minerals or an excessive amount of fat are then effectively excluded, regardless of their anatomical location.

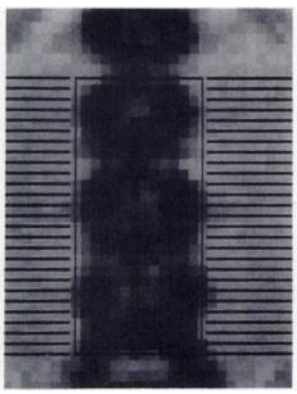

FIGURE 2
The rectangular region of interest comprises the vertebrae L2–L4. The soft-tissue baseline region (hatched area) is automatically selected and consists of all the pixels left and right of the region of interest.

Once the ROI has been placed onto the image by the operator, the program automatically selects all pixels left and right of the ROI that are within the upper and lower borders of the ROI (Fig. 2). A histogram is made of the "BMC" values of all selected soft tissue pixels (Fig. 3) and the median value is calculated. An area of this histogram is then selected, which starts with the values equal to the median and is expanded symmetrically until two thirds of the total pixels represented by the histogram are included. The average value of the selected pixels is calculated and compared to the median value determined before. If these values differ more than 0.5 U from each other, then another area is selected. This time the starting value is not the median value as in the first calculation, but a value 1 U closer to the calculated average of the pixels of the previous selection. The average of this new selection is again compared to this starting value. The above procedure is repeated until starting value and average value are within 0.5 U from each other. The average value of the last selection is used for baseline correction of all the pixels inside the ROI. Bone mineral content can now directly be calculated after subtraction of the final baseline value and division by the scaling factor C_2 (Equation 2).

Variations in the ST Baseline

In an ideal situation, with a homogeneous ST layer, the measured variations will be caused by the random nature of source decay and the chance of a photon to be detected. The detected intensities will show a Poisson distribution. The s.d. in the number of detected photons per pixel will then be equal to the square root of the mean number of counts. An approximation formula for calculating the s.d. of a general function y of the random variable x with a known s.d. was used to derive the formula for the s.d. in the ST baseline (*18*). The general approximation formula is:

$$SD(y) \approx \left(\frac{dx}{dy}\right)_{x=E(x)} \times SD(x). \quad (3)$$

In Equation 3, dy/dx is the derivative of y with respect to x, which is evaluated at the mean value of x. The file with the

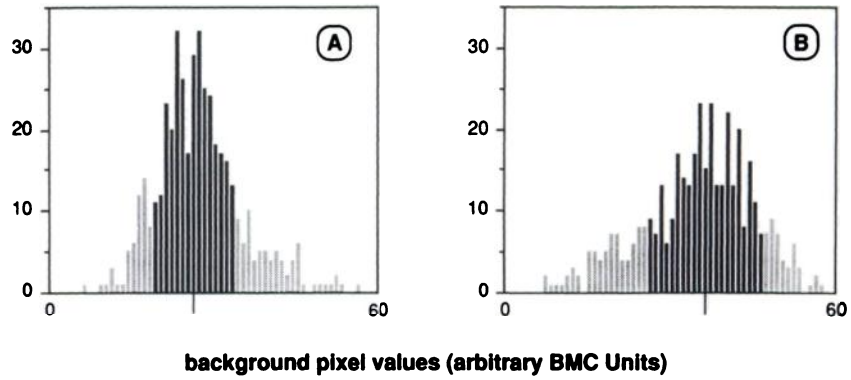

FIGURE 3
Histograms of the soft-tissue pixel values of a normal subject (A) and a patient with osteoporosis (B). The values which were excluded by the algorithm are depicted in grey. The center value of the selected portion of the histogram is marked at the horizontal axis. The width of the selected portion from the center value in either direction is used as estimation of the standard deviation of the soft-tissue baseline.

raw measurement data contains I^0_{44} and I^0_{100} at a soft tissue point lateral of the vertebral column, which have been measured during five seconds before the start of the actual scanning. Using the rearranged bone mineral Equation 2, the s.d. expressed in gHA can be calculated:

$$\text{Sd (gHA)} = \frac{0.16}{C_1} \times \sqrt{\frac{RST^2}{I^0_{100}} + \frac{1}{I^0_{44}}}. \quad (4)$$

The pixel values that are derived from the photon intensities show approximately a normal distribution. In practice, however, the measured variations in the ST layer can result from a combination of purely random error and anatomical variation. The width of the histogram of selected values is then a measure of the general variation in the soft tissue baseline, after exclusion of the extreme high and low values that disturb the approximately normal distribution (Fig. 3). An interval of one-third from the mean in either direction almost equals 1 s.d. in a set of values with a normal distribution, so half the width of the selected portion of the histogram that contains two thirds of the baseline values, might be a useful practical estimator of the s.d. in the representative part of the ST baseline.

The Estimation Error in BMC due to ST Variations

Calculation of the estimation error in the final BMC or BMD result, SE_{BMC} and SE_{BMD} respectively, is straightforward once the s.d. for the BMC per pixel is known. The final BMC value is calculated by subtraction of the mean baseline value from the mean uncorrected value inside the ROI, multiplied by the number of pixels inside the ROI. The mean uncorrected value consists of a mineral part and a ST part.

The estimation error of the mean value of the paravertebral baseline (SE_{ST}) is:

$$SE_{ST} = \frac{SD_{ST}}{\sqrt{N_{ST}}}, \quad (5)$$

where SD_{ST} is the s.d. in the ST BMC values and N_{ST} is the number of pixels outside the ROI that have been used to determine the ST baseline value. A similar equation gives SE_{ROI}, the estimation error of the ST part inside the ROI:

$$SE_{ROI} = \frac{SD_{ROI}}{\sqrt{N_{ROI}}}, \quad (6)$$

where N_{ROI} is the number of pixels inside the ROI and SD_{ROI} is the s.d. in the *ST part* of these pixels. However, SD_{ROI} cannot be directly measured, since variations in mineral mass are superimposed on the soft tissue variations. On the general assumption that the ST attenuation outside the ROI is representative for the ST attenuation inside the ROI, it may also be assumed that SD_{ROI} is essentially equal to SD_{ST} outside the ROI. The following equations will then be valid:

$$SE_{BMD} = SD_{ST} \times \sqrt{\frac{1}{N_{ROI}} + \frac{1}{N_{ST}}} \quad (7)$$

$$SE_{BMC} = SD_{ST} \times N_{ROI} \times \sqrt{\frac{1}{N_{ROI}} + \frac{1}{N_{ST}}} \quad (8)$$

Phantom Measurements

The agreement of the s.d. in baseline values estimated by the histogram method was compared with direct calculation of the s.d., using data from measurements in water layers with different heights. These s.d. values were also compared with the predicted s.d. for random error, calculated using Equation 4. The estimation error in the final BMC results of an aluminium tube due to these variations in the baseline was calculated using Equation 8. This tube has a BMC equivalent of 31.5 gHA measured with our system.

Since bone mineral absorbs more photons than ST, it must be expected that the random error related to count statistics will be larger inside the ROI than outside. A phantom study was performed to investigate whether this effect would have practical consequences. The dependency of s.d., expressed in BMD (g/cm^2), on the amount of mineral present in the photon beam was measured using an aluminum step phantom with 2-mm steps ranging from 2 mm through 10 mm thickness, immersed in 16 cm water. The intensities of both energies through the different aluminum steps were measured separately for 1 sec, with 25 measurements at each thickness. These measurements were repeated with the phantom in a water layer of 8 cm.

Measurements in Patients and Normal Subjects

The influence of the manual baseline selection procedure on the short-term precision error was investigated in 20 consecutive patients (18 women and 2 men, age 29–70 yr) routinely referred to our department. The scans of two women were excluded because of severe scoliosis. The source was 7-mo-old, with an estimated remaining activity of 2 GBq. The scans were analyzed twice by the same observer at different times using the original NOVO calculation software, version 1. The ROI in both analyses of the same patient was kept

TABLE 1
Variations in DPA Measurements of Water

Water depth	Detected counts		SD* per pixel (×0.0001 gHA)			SE-BMC (gHA)†	Predicted CV (%)‡
	44 keV	100 keV	Calculated	Measured	Histogram		
9 cm	15516	36476	31	34	29	0.10	0.31%
11 cm	9752	25988	38	41	43	0.12	0.37%
13 cm	6092	18588	47	52	43	0.15	0.48%
15 cm	3844	13472	58	60	57	0.18	0.57%
17 cm	2420	9596	71	70	71	0.21	0.69%

The results are expressed in equivalents of grams hydroxyapatite (gHA).
* The standard deviation (s.d.) of the values was calculated using the count rates, directly derived from the measurements, and estimated with the histogram method (see Patients and Methods section).
† SE-BMC is the estimation error in the final result of BMC, based on "Measured SD" and an average ROI.
‡ Coefficient of variation (CV) based on an aluminum phantom with a BMC equivalent of 31.5 gHA.

exactly the same, thus leaving the estimation of the baseline delimiters as the only variable.

The archived lumbar DPA scans of 57 patients with osteoporosis (45 women and 12 men, age 31–81 yr) were recalculated with the method described above, and the s.d. derived from the ST histogram was compared with the expected random error using the count rates in both channels at a ST point. These patients were scanned between April 1984 and September 1987 with four different gadolinium-153 sources. All sources had a nominal activity of 3.7 GBq and were changed at 13-mo intervals (June 1985, August 1986, September 1987) when the activity had fallen to one third of the nominal activity.

Thirteen patients with osteoporosis (11 women and 2 men, age 44–80 yr) underwent duplicate measurements of lumbar BMC. These measurements were performed in direct succession, with repositioning of the patient between the measurements. The s.d. of the ST baseline was determined and the mean estimation error in the final BMC was calculated. We compared this calculated error of estimation with the short-term precision error derived from the comparison of the duplicate measurements.

The same procedure as described above was followed using the archived lumbar scans of duplicate measurements in two groups of healthy volunteers (*17*). Ten subjects (5 women and 5 men, age 24–50 yr) were measured in direct succession with repositioning between their measurements. Eleven subjects (5 women and 6 men, age 23–49 yr) underwent their second measurement two hours after a standardized meal, containing 800 mg calcium and 750 mg phosphate from dairy products. This procedure was chosen to induce a maximal change in intestinal contents around the ROI, since ~60%–85% of the food will have passed the stomach in that period (*19*).

RESULTS

Phantom Measurements

Table 1 shows the results of the measurements of the variability of the baseline values with different heights of water. Using the number of counts in both channels, the expected random error was calculated with Equation 4. This calculated error agreed well with the s.d. derived from the measurements, indicating that with this ideal layer of ST the processes relating to source strength, absorber thickness and detection efficiency explain all the variance in the results. The estimation of the s.d. in baseline pixels with the histogram method was in agreement with both the calculated and measured results. Therefore, we chose this method to be used as estimator of the ST variability in the in vivo measurements.

The relation between increasing BMD of the step phantom and increase in s.d. is shown in Figure 4. We calculated the average s.d. for each thickness of aluminium in two ways. In the first calculation, the "BMD" was computed using the first part of Equation 2 with the counts in the high and low channels separately for each measurement. Then the s.d. was calculated in the 25 different results at each thickness. In the second

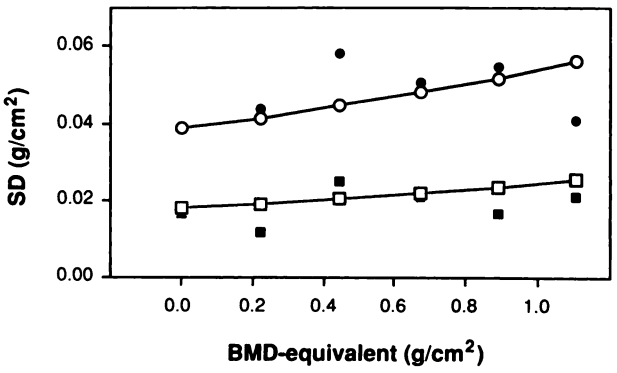

FIGURE 4
Measurements of calculated s.d. in BMD with increasing equivalents of BMD, simulated by five discrete steps of increasing aluminium thickness. Measurements of the aluminium phantom in 16cm water depth are depicted by open and closed circles, while measurements of the phantom in 8 cm water depth are depicted by open and closed squares. Two different ways of calculation yielded values for predicted s.d. (○ and □, connected by lines) and actual s.d. (● and ■). The scatter of the actual s.d. is large compared to the predicted effect of increasing BMD on s.d., thus in practice this effect is negligible.

calculation, we used the averaged count rates at each energy and each aluminum thickness, which were used in Equation 4 to derive a predicted s.d. for the different amounts of aluminium simulating bone mass. These results show that with a thin layer of water (high count rates) the predicted s.d. per pixel barely increased with increasing bone density equivalents from 0 g/cm^2 through 1.1 g/cm^2. Also with a thicker layer of water (lower count rates) there was only a moderate increase in predicted s.d. with increasing BMD.

The s.d. based on 25 measurements of 1 sec each, showed a scatter around the predicted line which, however, does not allow any more for the effect of increasing BMD on s.d. to be seen. In this way, BMD will have no detectable effect in the s.d. measurements obtained in practice and for this reason we decided not to include a correction for the amount of bone mineral inside the ROI in Equations 7 and 8, but assumed that the s.d. as measured in the paravertebral region is the same as the s.d. inside the ROI.

Measurements in Patients and Normal Subjects

The influence of the manual baseline selection procedure was based on 18 evaluable scans, twice evaluated with the standard calculation software. The overall mean BMC in these patients was 28.3 gHA, the precision error was 2.7%.

The s.d. in the ST background, estimated with the histogram method, was larger than the s.d. as expected from the count rates in all of the 57 archived patient scans (Table 2). Also with the duplicate measurements, in all patients as well as in all normals, higher values for ST s.d. were found with the histogram method than could be explained by random error. This shows that variations in the composition of the soft tissue baseline add to the random error in measurements in vivo.

Expressed in terms of gHA there was a slightly larger ST variation in patients than in normals (Table 2). The lowest s.d. was calculated for the group of 10 normals who were scanned twice in direct succession. This may be partially caused by the higher average count rates detected in this group. In the other group of normals, 11 subjects who had their second scan two hours after a meal, we found the lowest average count rates, but they showed also a significantly lower soft tissue s.d. than both groups of patients ($p = 0.01$. unpaired t-test).

In these 11 normal subjects, a slight increase of 9.1 $\times 10^{-4}$ gHA ($p < 0.05$, paired t-test) in the s.d. of the ST baseline pixels was also found (Table 3). However, the random error calculated using the count rates in ST did not change in comparison to the first scan. There were no changes in either random error or s.d. as calculated with the histogram method in the other group of normals and in the group of patients who had undergone duplicate scanning (Table 3).

Using Equation 8, we calculated the error in the BMC caused by the variations in the soft tissue baseline (Table 2). The resulting coefficient of variation (CV) was twice as large in the patients with osteoporosis than in the normal subjects. This was predominantly caused by the lower mean BMC in the patients and to a small degree by the slightly but significantly higher predicted estimation error expressed in gHA. The short-term reproducibility error of the duplicate measurements was larger than the predicted estimation error (Table 2), since extra variations were introduced by the placement of the ROI. The difference was larger in the patients than in the normal subjects.

DISCUSSION

Dual-photon absorptiometry is based on the assumption that bone mineral and the ST have a uniform composition. The BMC or BMD inside a ROI can be

TABLE 2
Variations in ST Values In Vivo with Lumbar DPA Measurements

	No. subjects	Detected counts (mean) 44 keV/100 keV	SD* per pixel (×0.0001 gHA) Calculated	SD* per pixel (×0.0001 gHA) Histogram	Predicted SE-BMC† (gHA)	Mean BMC (gHA)	Predicted CV (%)	Reproducibility based on duplicate scans (%)
Normal subjects								
Two successive scans	10	5036/17300	53 ± 12	99 ± 18‡	0.26 ± 0.07	40.5 ± 5.9	0.7%	1.6%
Meal between scans	11	3092/9992	67 ± 8	118 ± 16§	0.32 ± 0.06	44.7 ± 6.8	0.7%	1.5%
Patients								
Two successive scans	13	3348/11076	71 ± 32	135 ± 25‡§	0.37 ± 0.08	26.4 ± 8.5	1.5%	2.6%
Archived scans	57	4440/12556	65 ± 32	141 ± 25	0.36 ± 0.09	26.4 ± 6.5	1.4%	

The results are expressed in equivalents of grams hydroxyapatite (gHA). Means ± s.d. are shown.

* The standard deviation (s.d.) of the ST values were calculated using the count rates and were estimated with the histogram method (see Patients and Methods section).

† SE-BMC is the estimation error in the final result of BMC.

‡ $p < 0.0001$ (unpaired t-test).

§ $p < 0.02$ (unpaired t-test).

TABLE 3
Changes in ST Variability Between Duplicate Measurements

	No. subjects	Change in s.d.* per pixel (×0.0001 gHA)	
		Calculated	Histogram
Normal subjects			
Two successive scans	10	0.9 ± 5.4	−4.3 ± 6.9
Meal between scans	11	1.6 ± 5.8	9.1 ± 13.2†
Patients			
Two successive scans	13	0.8 ± 5.7	2.2 ± 20.9

The results are expressed in equivalents of grams hydroxyapatite (gHA). Means ± s.d. are shown.

* The s.d. of the ST values were calculated using the count rates and were estimated with the histogram method (see Patients and Methods section).

† $p < 0.05$ (paired t-test), comparison of second scan with first scan.

calculated if the attenuation characteristics of both bone mineral and ST are known. However, there may be considerable differences in the ratio of fat-to-lean tissue between individuals and within one person over a period of time. Hence, the attenuation characteristics of ST have to be determined in each DPA measurement separately. Its composition is assumed to be constant and the ST adjacent to the ROI is assumed to be representative for the ST inside the ROI. Based on these assumptions, an average value for the ST attenuation characteristics outside the ROI may be used to calculate BMC and BMD.

In addition to fat, a variable amount of calcified tissue (prominent transverse processes, calcified aorta, ribs, iliac crest) is present near the lumbar spine, causing further variations in the ratio of absorption of the high energetic and the low energetic photons in ST. Variations of this nature will occur inside the ROI, with a combination of bone mineral and ST, as well as outside the ROI where only ST is present. We show here that variations in composition of the paravertebral ST cause a s.d. in the baseline values, which is larger than can be explained by the count rates of the 44 keV and 100 keV photon beams. This eventually affects the reproducibility of the BMC results.

Our method of determination of the paravertebral baseline values has a number of potential advantages. First, it is an automatic method and therefore independent of the estimation of the baseline level by the operator as in the original calculation program (*12*). In this study, the effect of manual baseline selection on short-term precision was more than 2%, which emphasizes that manual selection of the baseline in patients with low BMC is difficult. Any automatic method would have no reproducibility error in this experiment, since the raw data and ROI were identical in both evaluations.

Second, inhomogeneity of the baseline, especially due to perirenal fat, is known to cause inaccurate estimation of the baseline (*11*). Conversely, mineral containing parts in the baseline region, such as the transverse processes, ribs, and various calcifications, can also cause false baseline values. A histogram of the baseline values reflects the numerical distribution of the values irrespective of their anatomical location in the baseline region. With perfectly homogeneous equivalents of ST, such as water in phantom measurements, the baseline values follow an approximately normal distribution. The only source of variation in such a system is the process of radioactive decay with a purely random nature. A histogram of the ST baseline values from a measurement in vivo reflects not only this random effect, but also the inhomogeneity of the absorption characteristics of the different tissues. Parts of the ST area that contain a relatively large amount of fat have a lower RST value. The "BMC" values of pixels from this area will be found in the left tail of the histogram. Mineral containing pixels will have values in the right tail of the histogram. The algorithm that we use to select a representative part of the baseline uses the central part of the histogram, comprising two-thirds of the number of baseline pixels. This fraction was chosen as a compromise to allow use of a relatively large number of values for determination of one average baseline value, while keeping low the number of outlying pixels in the selection. An iterative procedure selects those values that are symmetrically distributed around the peak of the histogram. With this procedure, the extreme values are excluded, even if the number of low values and high values differ considerably. In longitudinal measurements this is relevant, because with variations in repositioning different numbers of extreme values (e.g., ribs, pelvis) may appear in the baseline region. With straightforward calculation of the average, these extremes may have an unwanted large effect on the final baseline value. The exclusion of pixels is based on their values and not on their localization, thus no edge detection or threshold algorithms are needed in this procedure.

In measurements of water layers, half the width of the selected histogram closely correlated with the true s.d. of the baseline values. This was in agreement with the normal distribution of the values expected from the random nature of the variations. In a normal distribution, 68% of the values are comprised in the interval of two standard deviations centered around the mean. Although it is easy to calculate the s.d. of the baseline values in an ideal homogeneous layer, it is impossible to calculate it directly in vivo. The distribution of background values will be different in every measurement due to the anatomical variations and differences in intestinal contents. After the exclusion of the outlying values, the remaining part of the histogram has a similar

pattern as the central part of a normal distribution. Therefore, half the width of the selected interval of the baseline histogram can be used as an estimator of the s.d. in vivo.

In contrast to the close agreement of the estimated s.d. and the true s.d. in vitro, we constantly found a larger s.d. with the histogram method in vivo than predicted by the count rates in soft tissue. The difference between estimated s.d. and predicted s.d. was slightly larger in patients than in normals. We have no direct explanation for this phenomenon. The average age of the patients was higher than the age of the healthy subjects. Therefore, an increased amount of intraperitoneal fat, in major omentum and mesenterium, and an increased number of calcifications in veins and arteries may have been responsible. The increase in s.d. after a standardized meal was statistically significant but very small and of no practical consequence.

The estimation error in the final BMC calculation depends on the s.d. found in the ST baseline. Our results reveal an estimation error of 0.7% in normals and ~1.4% in patients with osteoporosis. This difference is mainly caused by the higher average BMC in normals (40.5 gHA) compared to patients with osteoporosis (26.4 gHA). However, it must be realized that this source of error is built up from the anatomical variation and the random error related to count statistics. Because our larger group of patients with osteoporosis was scanned over a period of more than three years with different sources, these results are adequate as average values. The number of photons reaching the detector is a function of ST thickness and source strength together. Soft-tissue thickness measured with our equipment (*16*) gives highly variable results, probably depending on the exact spot were the measurement is made. Therefore, it was not possible to quantify correlations between source strength and s.d. of the baseline or patient thickness and s.d. of the baseline separately.

In the calculations reported here other sources of error were not considered. The predicted estimation error was less than the reproducibility error assessed with duplicate measurements, both in normals and in patients. Positioning of the ROI and repositioning of the subject introduced an extra error, although the size of the rectangular ROI was the same in both scans of the same subject. In long-term follow-up scans, there will be more sources of error, such as equipment instability and source changes (*8,9*). Therefore, the predicted estimation errors derived in this study may be regarded as the limit of achievable precision with this particular bone densitometer. We believe that the other bone densitometers with gadolinium-153 radionuclide sources have equal limits of short-term reproducibility due to the variations in the ST baseline, since the principles of measurement are the same.

The most recent generation of bone densitometers is based on a calibrated dual-energy X-ray source of photons instead of a radionuclide source with its inherent disadvantages. One of the main features of these new instruments is the lower precision error (*20–24*). However, reported precision errors in measurements of human subjects are larger than in measurements of anthropomorphic moulded spine phantoms (*20,21*), suggesting that inhomogeneity of ST is also an important factor in achieving in vivo precision with dual-energy X-ray absorptiometry. The relative importance of this factor may be even greater because other sources of error such as source strength, equipment stability, and spatial resolution are much smaller than in the gadolinium-153-based machines.

ACKNOWLEDGMENT

This work has been presented at the EANM Congress, August 28 to September 1 1989, Strasbourg, France.

REFERENCES

1. Anonymous. Consensus development conference: profylaxis and treatment of osteoporosis. *BMJ* 1987; 295:914–915.
2. Riggs BL, Wahner HW, Melton LJ III, Richelson LS, Judd HL, Offord KP. Rates of bone loss in the appendicular and axial skeletons of women: evidence of substantial vertebral bone loss before menopause. *J. Clin Invest* 1986; 77:1487–1491.
3. Cummings SR, Black D. Should perimenopausal women be screened for osteoporosis? *Ann Intern Med* 1986; 104:817–823.
4. Genant HK, Block JE, Steiger P, Glueer CC, Ettinger B, Harris ST. Appropriate use of bone densitometry. *Radiology* 1989; 170:817–822.
5. Schaadt O, Bohr H. Bone mineral by dual-photon absorptiometry. Accuracy—precision—sites of measurements. In: Dequeker J, Johnston CC, eds. *Noninvasive bone measurements: methodological problems.* Oxford: IRL Press; 1982:59–72.
6. Krølner B, Berthelsen B, Pors Nielsen S. Assessment of vertebral osteopenia. Comparison of spinal radiography and dual photon absorptiometry. *Acta Radiol [Diagn]* 1982; 23:517–521.
7. Ross PD, Wasnich RD, Vogel JM. Magnitude of artifact errors in spine dual photon absorptiometry measurements. In: Christiansen C, Johansen JS, Riis BJ, eds. *Osteoporosis 1987.* Copenhagen: Osteopress ApS; 1987:389–391.
8. Dunn WL, Kan SH, Wahner HW. Errors in longitudinal measurements of bone mineral: effect of source strength in single and dual-photon absorptiometry. *J Nucl Med* 1987; 28:1751–1757.
9. Ross PD, Wasnich RD, Vogel JM. Precision error in dual-photon absorptiometry related to source age. *Radiology* 1988; 166:523–527.
10. Gotfredsen A, Pødenphant J, Nørgaard H, Nilas L, Herss Nielsen V-A, Christiansen C. Accuracy of lumbar spine bone mineral content by dual-photon absorptiometry. *J Nucl Med* 1988; 29:248–254.
11. Roos BO, Hansson T, Skoldborn H. Dual-photon absorptiometry in lumbar vertebrae. Evaluation of the baseline error. *Acta Radiol [Oncol]* 1980; 19:111–114.
12. Krølner B, Pors Nielsen S. Measurement of bone mineral

content (BMC) of the lumbar spine I. Theory and application of a new two-dimensional dual-photon attenuation method. *Scand J Clin Lab Invest* 1980; 40:653–663.
13. Krølner B. Lumbar spine bone mineral content by photon beam absorptiometry. *Dan Med Bull* 1985; 32:152–170.
14. Wahner HW, Dunn WL, Mazess RB, Towsley M, Lindsay R, Dempster A. Dual-photon Gd-153 absorptiometry of bone. *Radiology* 1985; 156:203–206.
15. Farrel TJ, Webber CE. The error due to fat inhomogeneity in lumbar spine bone mineral measurements. *Clin Phys Physiol Meas* 1989; 10:57–64.
16. Anonymous. *BMC-LAB22a Users handbook.* Bagsvaerd: NOVO Diagnostic Systems; 1983:62–67.
17. Valkema R, van den Berg R, Camps JAJ, et al. Precision of dual-photon absorptiometry measurements: comparison of three different methods of selection of the region of interest. *Eur J Nucl Med* 1989; 15:183–188.
18. Armitage P, Berry G. *Statistical methods in medical research,* Second edition. Oxford: Blackwell Scientific Publications; 1987:88–92.
19. Malmud LS, Fisher RS. Scintigraphic evaluation of esophageal transit, gastroesophageal reflux, and gastric emptying. In: Gottschalk A, Hoffer PB, Potchen EJ, eds. *Diagnostic nuclear medicine,* Second edition. Baltimore: Williams & Wilkins; 1988:663–686.
20. Wahner HW, Dunn WL, Brown ML, Morin RL, Riggs BL. Comparison of dual-energy x-ray absorptiometry and dual-photon absorptiometry for bone mineral measurements of the spine. *Mayo Clin Proc* 1988; 63:1075–1084.
21. Kelly TL, Slovik DM, Schoenfield DA, Neer RM. Quantitative digital radiography versus dual photon absorptiometry of the lumbar spine. *J Clin Endocrinol Metab* 1988; 67:839–844.
22. Mazess R, Collick B, Trempe J, Barden H, Hanson J. Performance of a dual-energy x-ray bone densitometer. *Calcif Tissue Int* 1989; 44:228–232.
23. Sartoris DJ, Resnick D. Dual-energy radiographic absorptiometry for bone densitometry: current status and perspective. *AJR* 1989; 152:241–246.
24. Cullum ID, Ell PJ, Ryder JP. X-ray dual-photon absorptiometry: a new method for the measurement of bone density. *Br J Radiol* 1989; 62:587–592.

EDITORIAL
Dual-Photon Absorptiometry in Clinical Practice

Osteoporosis is a descriptive diagnosis for bone that become sufficiently osteopenic such that fractures may occur spontaneously or with minimal trauma. There are numerous etiologies for osteopenic bone. This is not just a disease of postmenopausal females. The most serious consequences of weakened bones—vertebral crush fracture and hip fracture—approach ten billion dollars in direct, acute health care costs annually in the United States. This figure does not include the costs associated with long-term custodial care, required for a large portion of patients who suffer hip fractures later in life. Twenty percent of patients who suffer hip fracture over age 45 will die within a year of their fracture and at least half of those who were ambulatory before fracture cannot walk independently following hip fracture. The life-time risk of hip fracture in white women is 15% and 5% for white men. If we could extend by five or six the number of postmenopausal years for women before hip fracture occurs, we could cut the total number of fractures in half (*1*).

Vertebral fractures occur earlier in life than hip fractures and are medically significant themselves in terms of back pain, decreased physical activity, and change in physical appearance. Loss of height secondary to the development of senile dorsal kyphosis may result in disabling psychologic problems because of altered physical appearance and fear of fracture. The cost of this loss of independence is incalcuable.

Methods to assess bone density as a measure of bone strength and fracture likelihood have been available since 1963 (*2*). The past decade has brought us increasingly accurate and precise methods for determining bone density. However, because osteoporosis is generally a disease of slow progression, response to therapy or progression of disease are both difficult to gauge in short time frames. Thus, diagnostic precision is extremely important for any procedure used to follow response to therapy of osteoporosis.

Previous articles in *The Journal of Nuclear Medicine* have addressed both the precision (*3*) and accuracy (*4*) of dual-photon absorptiometry (DPA) of the spine in the diagnosis of osteoporosis. The article by Valkema and colleagues in this issue of the *Journal* (*5*) is a further contribution to our understanding of those technical factors which may effect the precision of DPA as applied to patients. Measurements in both volunteers and patients showed greater variation than measurements of bone mineral content obtained by the use of a water phantom. They found a greater variation in soft-tissue baseline than expected beyond random error. The effect on short-term precision was greater than 2%. They ascribed this source of error to the inhomogeneity of soft tissue, resulting in a standard deviation in the baseline values larger than could be explained by the

Received Aug. 17, 1990; accepted Aug. 17, 1990.
For reprints contact: Ralph G. Robinson, MD, Division of Nuclear Medicine, Department of Diagnostic Radiology, Kansas University Medical Center, Kansas City, Kansas 66103.